JEE Journal of Ecological Engineering

Journal of Ecological Engineering, 2026, 27(7), 256–272
https://doi.org/10.12911/22998993/218786
ISSN 2299–8993, License CC-BY 4.0

Received: 2026.02.05
Accepted: 2026.05.15
Published: 2026.06.01

Sustainable production of graphene oxide derived from sugarcane bagasse for dispersive solid phase extraction

Rinawati[1*], Dian Rifani Muthia[1], Geby Tiorya Angelina Manurung[1], Aranca Putri Maharani S.[1], Elsa Fitrianingsih[1], Suharso[1], Agung Abadi Kiswandono[1], Fahamsyah Hamdan Latief[2], Widiarti[3]

[1] Departement of Chemistry, Universitas Lampung, Bandar Lampung 35145, Indonesia
[2] Department of Mechanical Engineering, Universitas Nasional, Jakarta 12520, Indonesia
[3] Department of Mathematics, Universitas Lampung, Bandar Lampung 35145, Indonesia
* Corresponding author's e-mail: rinawati@fmipa.unila.ac.id

ABSTRACT

The ubiquitous prevalence of ciprofloxacin (CIP) in aquatic environments has prompted concerns about its durability, ecological effect, and contribution to antimicrobial resistance. To address this difficulty, analytical extraction procedures must be both sensitive and environmentally friendly. This paper describes a green dispersive solid-phase extraction (DSPE) method for CIP determination that uses graphene oxide (GO) derived from sugarcane bagasse as a renewable biomass precursor. GO was synthesized in a single step using a low-temperature thermal technique and then characterized using FTIR, SEM-EDX, and XRD, showing the successful production of oxygen-rich and structurally disordered GO suited for adsorption applications. The DSPE parameters were systematically tuned using response surface methodology (RSM) with a Box-Behnken design (BBD) to investigate the effects of pH, GO mass, and contact time on CIP adsorption efficiency. The quadratic model well represented adsorption behavior, with a high coefficient of determination ($R^2 = 0.9726$) and great prediction dependability. GO mass was found to be the most influential factor, with pH and contact duration serving as secondary parameters that fine-tuned the adsorption process. Under optimal conditions (pH 3.16, GO mass 43.00 mg, contact time 29.94 min), the model projected a 90.46% CIP adsorption efficiency. The experimental validation resulted in an average adsorption of 88.39%, with a small prediction error of 2.34%, demonstrating excellent agreement between anticipated and experimental results. These findings show that sugarcane bagasse-derived GO is a very effective and sustainable adsorbent for DSPE-based CIP analysis, providing a dependable platform for monitoring trace antibiotics in aquatic systems.

Keywords: graphene oxide, ciprofloxacin, dispersive solid phase extraction, response surface method.

INTRODUCTION

Antibiotic residues in aquatic environments are a global environmental and public health issue. The widespread use of antibiotics in human, veterinary, animal, and aquaculture causes leakage into surface, groundwater, and wastewater systems (Bansal, 2022; Barathe et al., 2024; Berisha et al., 2024). Ciprofloxacin (CIP), a fluoroquinolone antibiotic used to treat bacterial infections, is one of the most regularly discovered chemicals in traditional wastewater treatment plants due to its high chemical stability, poor metabolization, and low removal efficiency (Imam et al., 2023; Yakamercan et al., 2024). Continuous CIP pollution has been shown to cause antimicrobial-resistant bacteria, impair aquatic endocrine regulation, and cause long-term ecological imbalance, threatening environmental sustainability and public health (Sharma, 2025; Wang et al., 2023). Thus, accurate and sensitive trace-level CIP measurement in aquatic settings is essential for environmental monitoring and risk assessment.

Due to its low concentration and the complexity of aqueous matrices containing organic and inorganic interferents, CIP identification in environmental samples is difficult (David et al., 2019). Sample preparation is crucial for detection

sensitivity and analytical reliability in these cases. Based on its operational simplicity, quick extraction kinetics, reduced solvent consumption, and green analytical chemistry principles, dispersive solid-phase extraction (DSPE) has gained popularity as a sample preparation method (Ścigalski and Kosobucki, 2020; Silveira et al., 2019; Shukri et al., 2023). DSPE improves mass transfer between the analyte and adsorbent over solid-phase extraction, increasing extraction efficiency and reducing processing time (Hagarová and Nemček, 2024; Taghvimi et al., 2020). The physicochemical parameters of the adsorbent material greatly affect DSPE performance.

Graphene oxide (GO) has emerged as a promising adsorbent for antibiotic extraction due to its extensive specific surface area, hydrophilicity, and the presence of numerous oxygen-containing functional groups, including hydroxyl, epoxy, and carboxyl moieties Salihi et al., 2021; Ahmmed and Mohiuddin, 2024. These functional groups engage with fluoroquinolone antibiotics via hydrogen bonding, electrostatic attraction, and π-π interactions, allowing for effective CIP adsorption from aqueous solutions (Li et al., 2018; Umeh et al., 2025; Yadav et al., 2018). Such characteristics are essential for an effective solid adsorbent phase in DSPE, thereby supporting its application in analytical sample preparation. However, GO is still not commonly employed because existing methods of production use nonrenewable graphite precursors and require expensive, chemically intense, and environmentally destructive processes (Edward et al., 2023; Silva et al., 2024). These limits have prompted increased research into the production of GO derived from renewable, cost-effective, and environmentally friendly biomass materials (Buhani et al., 2017; Rinawati et al., 2023).

Recent studies show that graphene-based or graphene-like materials can be effectively generated from diverse agricultural wastes, such as cassava peels, corn cobs, and coconut shells, and subsequently utilized as antibiotic adsorbents (Sujiono et al., 2020; Rinawati et al., 2024). These results endorse the utilization of agricultural byproducts as an alternative carbon source for graphene-based goods. Mostearlier study, however, have focused on batch adsorption techniques for pollution removal rather than analytical extraction at trace levels. Moreover, researchers have inadequately investigated the application of biomass-derived graphene materials in DSPE systems and the systematic adjustment of extraction parameters for analytical determination. Consequently, the amalgamation of regionally abundant agricultural byproducts with sustainable analytical methodologies represents a crucial yet underexplored domain of research (Cardoso et al., 2024; Li et al., 2024).

Sugarcane bagasse, the primary product of the sugar industry, is a good source of carbon because it is fibrous, has around 50% carbon content, and is easy to find (Torgbo et al., 2021; Mubarak et al., 2024). Lampung Province in Indonesia is one of the biggest sugar-producing locations in the country. Each year, it makes a lot of sugarcane bagasse. This biomass waste is underutilized and often discarded in low-value applications or burned in the open, harming the environment. Transforming sugarcane bagasse into GO is a sustainable way to make use of agricultural waste. It fits with the ideas of the circular economy and encourages environmentally friendly material development (Somanathan et al., 2015; Thangaraj et al., 2023). The utilization of GO produced from sugarcane bagasse as an adsorbent for DSPE-based antibiotic analysis remains insufficiently investigated in the literature, despite its significant potential.

Building on this identified research gap, the performance of DSPE is influenced by several key operational parameters, including solution pH, adsorbent dose, extraction time, and desorption conditions (Socas-Rodríguez et al., 2015; Oner et al., 2023). Conventional one-factor-at-a-time approaches are inefficient and fail to capture interactions between variables. Therefore, response surface methodology (RSM), particularly Box–Behnken design (BBD), is widely applied as a statistically efficient tool to optimize multiple parameters simultaneously with a reduced number of experiments

MATERIALS AND METHODS

Materials

The materials used in this study included sugarcane bagasse from PT. Gunung Madu Plantations in Indonesia, which served as the primary biomass precursor for GO synthesis; ferrocene purchased from Supelco Sigma Aldrich; ciprofloxacin analytical standard supplied by Hexpharm Jaya; hydrochloric acid (37%) and glacial acetic acid obtained from Smart Lab; sodium hydroxide purchased from Merck; and distilled water, which was used throughout all experiments.

Single-step synthesis of GO

The sugarcane bagasse utilized in this study was sourced from local producers in Bandar Lampung, Lampung Province, Indonesia, and collected during a single harvest season to maintain consistency in its physicochemical properties. Sugarcane bagasse was initially subjected to a thorough cleaning with distilled water to remove surface impurities and residual contaminants. The material was air-dried in sunlight for 2–3 days and then oven-dried at 80 °C for 5 hours to ensure the complete removal of residual moisture. The dried bagasse was finely ground into a homogeneous powder, placed in a ceramic crucible, and carbonized in a muffle furnace at temperatures of 400, 500, and 600 °C for 1 hour under air atmosphere, with an estimated heating rate of approximately 20 °C/min, yielding carbonized bagasse.

In the synthesis of GO, 5 g of carbonized bagasse was uniformly mixed with ferrocene at mass ratios of 0.5, 1.0, and 1.5. The mixtures were placed in ceramic crucibles and subjected to thermal treatment in a furnace at 300 °C for 10 minutes under air atmosphere. This controlled thermal process facilitated the formation of GO via a single-step synthesis route, producing biomass-derived GO appropriate for subsequent analytical applications. No additional washing or purification steps were applied after synthesis.

Characterization methods of GO

The surface functional groups of the produced GO were carefully examined with Fourier transform infrared spectroscopy (FTIR) to detect the presence of oxygen-containing functionalities. Scanning electron microscopy coupled with energy dispersive x-ray analysis (SEM-EDX) was used to thoroughly evaluate the material's morphological features and elemental makeup. Furthermore, the crystalline structure and phase characteristics of the produced GO were assessed using x-ray diffraction (XRD) to determine structural ordering and phase composition.

CIP adsorption test

The adsorption process was directly optimized RSM, where pH, contact time, and adsorbent mass were treated as independent variables. In an adsorption experiment, GO was added to a beaker holding 20 mL of a CIP standard solution at a concentration of 4 ppm selected as a representative concentration for the adsorption study, while the pH was adjusted according to the RSM design. The mixture was stirred for the contact time specified by the RSM matrix to ensure adequate interaction between the adsorbent and the analyte.

After the adsorption process, the GO was separated by centrifugation at 10.000 rpm for 15 minutes. The supernatant was then filtered to remove any remaining particles, and the filtrate was analyzed using a UV–Vis spectrophotometer at the maximum absorption wavelength of CIP.

Optimization of DSPE using RSM

The DSPE technique was optimized utilizing RSM with a BBD. Four independent variables were selected: GO mass, solution pH, and contact time. Table 1 summarizes the evaluation of each factor at three coded levels: low (-1), medium (0), and high (+1). The experimental design matrix was created with Design Expert software version 13.0, yielding a total of 29 experimental runs.

The percentage of c CIP adsorption was set as the response variable for each experimental run. To determine the relevance of individual factors and their interactions, the experimental data were statistically evaluated using analysis of variance (ANOVA). The fitted response surface models were then utilized to create three-dimensional response surface plots, allowing for the visualization of interaction effects and the discovery of optimal DSPE settings for CIP adsorption employing GO as an adsorbent (Gupta et al., 2017).

The BBD experimental matrix dictated that all trials be carried out sequentially. In each run, a CIP solution of a specific concentration was combined with a predetermined amount of GO under pH and contact time controls. After the adsorption process was completed, the adsorbent was removed from the solution using centrifugation and then filtration. A UV-Vis spectrophotometer with a wavelength of 278 nm was used to quantify the residual CIP content in the filtrate. Equation 1 and 2 was used to computse the yield percentage and adsorption efficiency:

$$\%yield = \frac{Mass\ of\ obtained\ GO}{Initial\ mass\ of\ graphite} \times 100\% \quad (1)$$

$$Adsorption\ (\%) = \frac{Co - Cx}{Co} \times 100 \quad (2)$$

where: C_o denotes the starting concentration of CIP (μg mL^{-1}) and Cx indicates the ultimate concentration following adsorption (μg mL^{-1}).

The established RSM model's predictive ability was evaluated by computing the percentage error between experimentally observed values and model-predicted values using Equation 3.

$$\%\ Error = \left|1 - \frac{Prediction\ Value}{Experiment\ Value}\right| \times 100\% \quad (3)$$

The experimental design for DSPE optimization was formulated using a BBD featuring three coded levels for each variable: low (−1), middle (0), and high (+1). Three independent variables were evaluated: GO adsorbent mass, solution pH and contact duration, as detailed in Table 1. The CIP concentration was fixed at a representative level to simplify the model and focus on key operational variables, consistent with common RSM-based adsorption studies (Zhao et al., 2023). The experimental matrix was created with Design Expert software version 13.0, yielding a total of 17 experimental runs, as shown in Table 2. The percentage of CIP adsorption derived from the DSPE studies was designated as the response variable and later assessed using ANOVA. The response data were further analyzed by RSM to determine the best DSPE settings for CIP adsorption utilizing GO as the adsorbent (Gupta et al., 2017).

All tests were conducted progressively following the BBD experimental matrix. In each experiment, a CIP solution of a designated concentration was combined with a given quantity of GO under regulated pH and contact time parameters. Subsequent to the adsorption process, the adsorbent was isolated from the solution using centrifugation and subsequent filtration. The residual concentration of CIP in the filtrate was measured using a UV–Vis spectrophotometer at a wavelength of 278 nm, and the adsorption efficiency was determined as the response variable in accordance with Equation 1.

RESULTS AND DISCUSSION

Single-step synthesis of GO

The synthesis of GO from sugarcane bagasse waste encompassed four sequential preparation phases: washing, drying, grinding, and carbonization. Each phase is essential for evaluating the quality of the resulting carbon precursor. Figure 1 illustrates the visual progression of these stages. Figure 1a illustrates that the raw sugarcane bagasse underwent an initial washing process to eliminate adhering soil, residual sugars, and other surface impurities that could affect subsequent heat treatment. This cleaning step is crucial for reducing inorganic contaminants and facilitating a more consistent carbonization process. After the effective washing, the bagasse was dried, as seen in Figure 1b, to eliminate moisture content, avert adverse reactions during heating, improve grinding efficiency, and promote uniform thermal decomposition.

Table 2. Box–Behnken experimental design for DSPE optimization

Run	pH	GO adsorbent mass (mg)	Contact time (min)
1	5	50	60
2	5	30	35
3	2	30	10
4	5	30	35
5	8	10	35
6	5	10	10
7	5	10	60
8	2	50	35
9	8	30	60
10	5	30	35
11	2	10	35
12	2	30	60
13	5	50	10
14	5	30	35
15	8	30	10
16	8	50	35
17	5	30	35

Table 1. Independent variable levels in the BBD design

Factor	−1 (Low)	0 (Center)	+1 (High)
GO adsorbent mass (mg)	10	30	50
Solution pH	2	5	8
Contact time (min)	10	35	60

The dried bagasse was milled into a fine powder (Figure 1c), augmenting the surface area and enhancing particle size homogeneity; hence, it promoted constant heat transmission during carbonization. The carbonization process produced a black carbonaceous solid (Figure 1d), signifying substantial structural and compositional alterations in the lignocellulosic biomass. The noted color change and textural modification indicate effective thermal degradation and the formation of a carbon-rich matrix, thus validating the material's appropriateness as a precursor for further transformation into GO.

After carbonization, the bagasse was carefully pulverized and sieved through a 100-mesh screen to achieve a uniform particle size. This procedure facilitated the incorporation of ferrocene and ensured consistent heat transfer throughout the thermal process. Five grams of carbonized material were methodically mixed with one gram of ferrocene ($Fe(C_5H_5)_2$), acting simultaneously as a catalyst and a functionalizing agent. The mixture was subsequently heated to 300 °C for 15 minutes to promote surface modification and enhance the yield of GO. Under these conditions, ferrocene decomposes into iron-based active species that promote the activation and oxidation of the surface, especially at defect sites and margins of the carbon matrix. This leads to the development of functional groups containing oxygen, such as hydroxyl, carbonyl, and epoxide groups (Tamilselvi et al., 2020).

Furthermore, Figure 1d demonstrates the efficacy of the ferrocene-assisted heating procedure. The result is a consistent, black substance that visually distinguishes itself from the original material employed in its synthesis. The uniform coloration and granular consistency suggest successful modification of the carbon surface and structural disintegration, in line with the development of an oxidized carbon material appropriate for adsorption. The 83.22% yield demonstrates efficient conversion at low temperatures with minimal material loss, thereby confirming the technique as an effective method for producing GO from biomass.

Characterization of the prepared GO

Figure 2 shows the FTIR spectra of graphite derived from sugarcane bagasse, GO derived from sugarcane bagasse, and GO derived from commercial graphite, highlighting the chemical changes during oxidation.The graphite derived from sugarcane bagasse (Figure 2a) displays a broad band at 3200–3250 cm^{-1} attributed to O–H stretching from residual hydroxyl groups and adsorbed moisture, along with a weak band near ~1700 cm^{-1} corresponding to limited carbonyl (C=O) functionalities (Darmawan et al., 2024; Supriyanto et al., 2018). These features indicate slight surface oxidation despite the predominantly aromatic carbon structure. Unlike pristine mineral graphite, biomass-derived carbon typically retains oxygen-containing groups due to partial oxidation and incomplete removal of oxygenated components during carbonization, explaining the presence of O–H and C=O bands (Sayfo et al., 2023; Yang et al., 2022).

Conversely, GO derived from sugarcane bagasse (Figure 2b) shows a heightened quantity of oxygen-containing functional groups. The O–H stretching band at approximately 3250 cm^{-1} is more pronounced and broader, signifying an increased abundance of hydroxyl groups on the carbon surface (Thangaraj et al., 2023). The absorption band at about 1700 cm^{-1} is associated with the stretching vibrations of C=O bonds in carbonyl and carboxyl groups (Darmawan et al., 2024; Poonpat et al., 2025). Supplementary bands in the 1200–1100 cm^{-1} range result from the stretching vibrations of C–O and C–O–C bonds, signifying the presence of epoxy and alkoxy groups. Meanwhile, Figure 2c illustrates that the FTIR

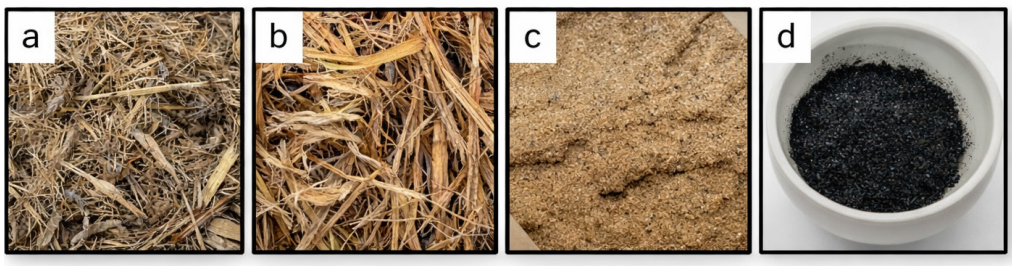

Figure 1. Sequential preparation steps of sugarcane bagasse for GO synthesis: (a) cleaned bagasse, (b) dried bagasse, (c) milled bagasse powder, and (d) carbonized bagasse

Table 3. FTIR result

Sorbent	Functional group (cm^{-1})				
	-OH	C=O	C=C	C-O-C	C-O
Graphite-derived sugarcane bagasse	3204	1700	1570	-	-
GO- derived sugarcane bagasse	3253	1700	1579	1095	1216
GO-Flake	3175	1722	1610	1058	1237

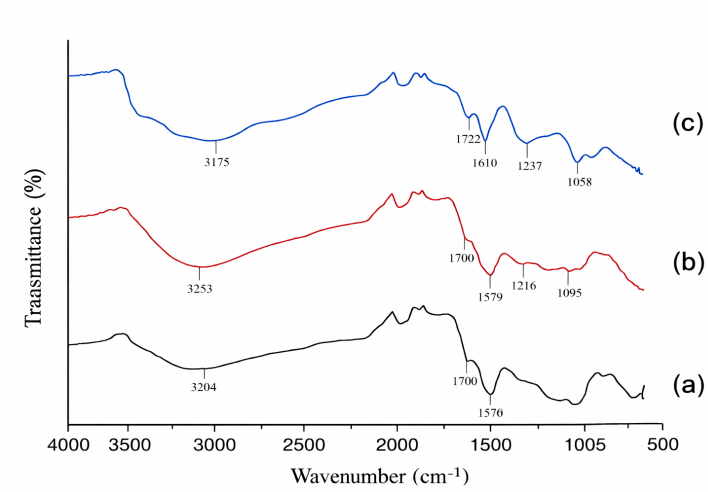

Figure 2. FTIR spectra of (a) graphite-derived sugarcane bagasse, (b) GO-derived sugarcane bagasse, and (c) GO-derived commercial graphite

spectrum of GO commercially graphite exhibits prominent O–H, C=O, and C–O absorption bands indicative of GO. Although synthesized via several techniques and from distinct sources, the spectrum of GO obtained from sugarcane bagasse roughly mimics that of GO-commercial graphite (Challa et al., 2022).

Figure 3 shows images taken with SEM that show the different shapes of GO made from sugarcane bagasse and commercial GO. Both materials have sheet-like structures that are typical of GO, but there are clear changes in the texture of the surface and the way the structures are organized. Figure 3a shows that sugarcane bagasse GO is made up of sheets that are not straight, have wrinkles, and are only partially folded. The surface is also rather rough. The overlapping layers and deep wrinkles show that the structure is heterogeneous and has many defects. This type of structure is characteristic for biomass-derived GO made by mild thermal oxidation. These kinds of morphological features make the surface rougher and show more edge sites, which is advantageous for applications that rely on adsorption (Zhu et al., 2015). The summary of functional groups on each sorbent is presented in Table 3.

In Figure 3b, commercial GO shows sheets that are thinner and more even, with smoother surfaces and a well-defined platelet-like shape. The better layer uniformity indicates a higher level of exfoliation and structural ordering, which usually happens when chemical oxidation is done in a regulated way. This shape makes the structure more stable, but the smoother surface suggests that there are fewer active spots connected to defects than in sugarcane bagasse GO (Nishina, 2024).

The elemental composition of GO produced from sugarcane bagasse and commercial GO was determined using Energy Dispersive X-ray (EDX) analysis, as seen in Figure 4. Figure 4a shows that the GO produced from sugarcane bagasse has 62.92 wt% C and 37.04 wt% O. The presence of considerable oxygen content shows that oxygen-containing functions were successfully integrated during ferrocene-assisted thermal treatment. The wrinkled and defect-rich appearance observed in SEM lends support to the theory that oxidation occurs largely at edge sites and structurally disordered portions of the carbon framework. The

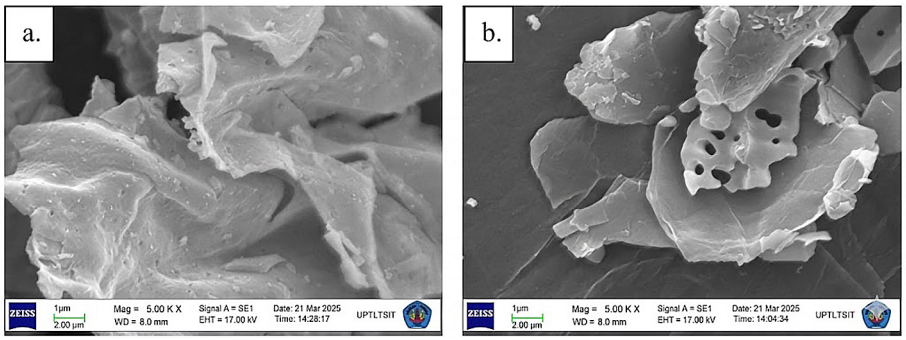

Figure 3. SEM images of (a) GO-derived sugarcane bagasse and (b) GO- derived commercial graphite

resulting surface chemistry contains polar functional groups that facilitate interactions with target molecules during adsorption processes (Ariyanti et al., 2021). Commercial GO (Figure 4b) has an elemental makeup of 59.85 wt% C and 40.59 wt% O, indicating a slightly higher level of oxidation. The higher oxygen concentration is consistent with the uniform and exfoliated sheet shape observed in SEM, indicating a synthesis approach that allows for more uniform surface functionalization across the GO sheets (Laçin et al., 2022).

The XRD patterns in Figure 5 reveal the structural alteration of sugarcane bagasse-derived carbon throughout oxidation and allow for direct

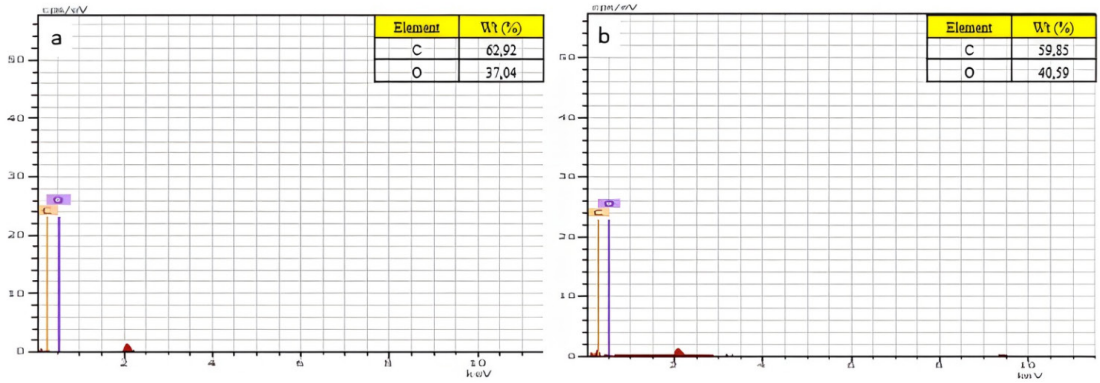

Figure 4. EDX spectra of (a) sugarcane bagasse-derived GO and (b) commercial GO

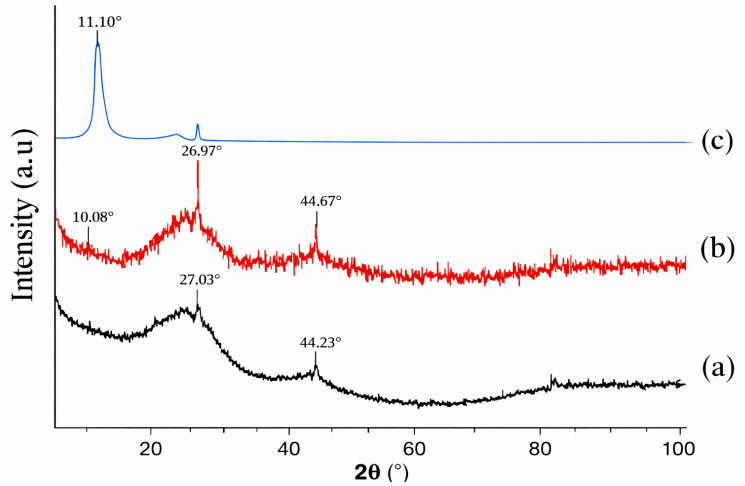

Figure 5. XRD patterns of (a) sugarcane bagasse-derived graphite, (b) sugarcane bagasse-derived GO, and (c) commercial GO

comparison with commercial GO. The diffraction pattern of sugarcane bagasse graphite (Figure 5a) is characterized by a large peak centered at 2θ = 27.0°, representing the (002) reflection of graphitic carbon. The strong peak broadening implies a turbostratic and disordered structure, which is typical of biomass-derived graphite generated during carbonization. A faint reflection at 44.2° along the (100) plane supports the presence of disordered graphitic domains rather than well-developed crystalline graphite. Besides, the XRD pattern of sugarcane bagasse GO changes significantly when oxidized (Figure 5b). A new diffraction characteristic occurs at lower angles around 2θ = 10.1°, indicating a widening of interlayer space due to the inclusion of oxygen-containing functional groups and intercalated species between carbon layers. At the same time, a weak and widened peak remains at about 26–27°, showing that some of the original graphitic structure is still there (Somanathan et al., 2015; Mohamed et al., 2024). The presence of enlarged GO layers and remnant graphitic domains indicates a heterogeneous layered structure, which is prevalent in GO created by mild or single-step oxidation methods.

The XRD pattern of commercial GO (Figure 5c) shows a strong and powerful diffraction peak at roughly 2θ = 11.1°, indicating well-oxidized GO and uniformly increased interlayer spacing. The lack of a discernible peak near 26° indicates significant disruption of the original graphite stacking and a more homogenous oxidation process. This structural consistency reflects the stronger and more regulated oxidation conditions commonly used in conventional GO production.

Optimization of DSPE using RSM

Statistical analysis

Table 4 shows that CIP adsorption by GO varies greatly, ranging between 58.9% and 90.3%, demonstrating a substantial dependency on operating circumstances. The highest adsorption is attained at pH 2 with 50 mg GO and 35 minutes of contact time (Run 8, 90.31%), whereas the lowest adsorption occurs at pH 5 with 10 mg GO and 10 minutes (Run 6, 58.86%). Among the tested factors, GO mass has the greatest influence on adsorption efficiency. Increasing adsorbent mass from 10 mg to 50 mg reliably improves CIP removal, regardless of pH or contact time, due to the increased availability of active adsorption sites and effective surface area (Ahmmed et al., 2024). When the GO mass is minimal, adsorption is limited even under favorable pH conditions, showing that site availability is the primary limiting factor.

Once a substantial amount of GO mass is present, the effects of pH and contact duration become apparent. Higher adsorption at acidic pH,

Table 4. Ciprofloxacin (CIP) adsorption efficiency using GO as adsorbent under different DSPE conditions

Run	pH	GO mass (mg)	Contact time (min)	CIP adsorption (%)
1	5	50	60	79.77
2	5	30	35	84.09
3	2	30	10	85.11
4	5	30	35	82.83
5	8	10	35	60.26
6	5	10	10	58.86
7	5	10	60	61.65
8	2	50	35	90.31
9	8	30	60	80.18
10	5	30	35	89.52
11	2	10	35	59.01
12	2	30	60	81.15
13	5	50	10	85.48
14	5	30	35	88.13
15	8	30	10	82.69
16	8	50	35	85.48
17	5	30	35	83.67

at pH 2, indicates favorable interactions between CIP and oxygen-containing functional groups on the GO surface, which are supported by both electrostatic and non-electrostatic interactions. Contact time exhibits a non-monotonic effect, with intermediate durations consistently outperforming the shortest and longest timeframes, showing that fast adsorption is followed by surface rearrangement or partial re-equilibration. Replicated center-point experiments at pH 5, 30 mg GO, and 35 minutes produce adsorption values with low variability, indicating good experimental reproducibility and giving a solid foundation for further RSM modelling (Bruckmann et al., 2024). The results indicate that optimal CIP adsorption is achieved through the combination of a suitable adsorbent mass, an adequate pH, and a moderate contact duration, aligning with the criteria for a successful DSPE process.

The statistical summary in Table 5 demonstrates that the quadratic model best represents the DSPE adsorption system. The highly significant sequential p-value ($p = 0.0004$) demonstrates that including second-order factors enhances the model beyond basic linear correlations. At the same time, the non-significant lack-of-fit value ($p = 0.5932$) demonstrates that the quadratic model accurately represents the observed variability, with no systematic deviations. In contrast, the linear and two-factor interaction (2FI) models show substantial lack-of-fit, showing that they cannot represent the non-linear nature of the adsorption process.

The quadratic model's high adjusted R^2 (0.9373) and anticipated R^2 (0.8190) show significant agreement between experimental and predicted responses, indicating reliable predictive performance in the analyzed design space. The relatively modest discrepancy between these two values indicates high model stability with minimal overfitting. The linear and 2FI models have lesser explanatory power, with the Two-Factor Interaction (2FI) model predicting a negative R^2, indicating poor predictive dependability. The cubic model is aliased due to experimental design constraints and so cannot be comprehended. These findings demonstrate that CIP adsorption onto GO is regulated by nonlinear effects, making the quadratic model the best framework for response surface optimization and analysis (Fernandi et al., 2015).

The quadratic model's adequacy was evaluated using diagnostic plots, as shown in Figure 6, to ensure that the statistical assumptions required for reliable prediction were met. Figure 6a demonstrates that the residuals are distributed closely along the diagonal line, indicating that they have an approximately normal distribution. This pattern demonstrates that the differences between experimental and predicted values are random and that the model fits the data perfectly, which is consistent with prior RSM-based investigations (Anggraini et al., 2023).

The predicted versus actual plot (Figure 6b) indicates the model's high predictive performance. The majority of data points are near to the diagonal line, indicating a high degree of agreement between experimental results and model predictions. This close match confirms the quadratic model's high coefficient of determination and demonstrates that the model successfully reflects the variability of the CIP adsorption response. Similar diagnostic patterns have been observed in comparable adsorption experiments, where significant congruence between predicted and experimental values indicates accurate model performance (Anggraini et al., 2023).

The residuals vs. run plot (Figure 6c) reveals a random distribution of residuals around the zero line, with all points remaining within the control limits and no discernible trends between experimental runs. This trend demonstrates the absence of systematic error, time-dependent effects, or experimental bias, as well as the dataset's constant variance. Together, these diagnostic results show that the quadratic model is statistically valid and suitable for forecasting CIP adsorption within the experimental range investigated (Fernandi et al., 2015). This validated model yielded a quadratic polynomial equation characterizing the CIP adsorption

Table 5. Statistical summary of model fitting for DSPE optimization using RSM

Model	Sequential p-value	Lack-of-Fit p-value	Adjusted R^2	Predicted R^2	Model status
Linear	0.0025	0.0294	0.5757	0.4124	Not adequate
2FI	0.9328	0.0163	0.4709	-0.1417	Not adequate
Quadratic	0.0004	0.5932	0.9373	0.8190	Selected
Cubic	0.5923	-	0.9285	-	Aliased

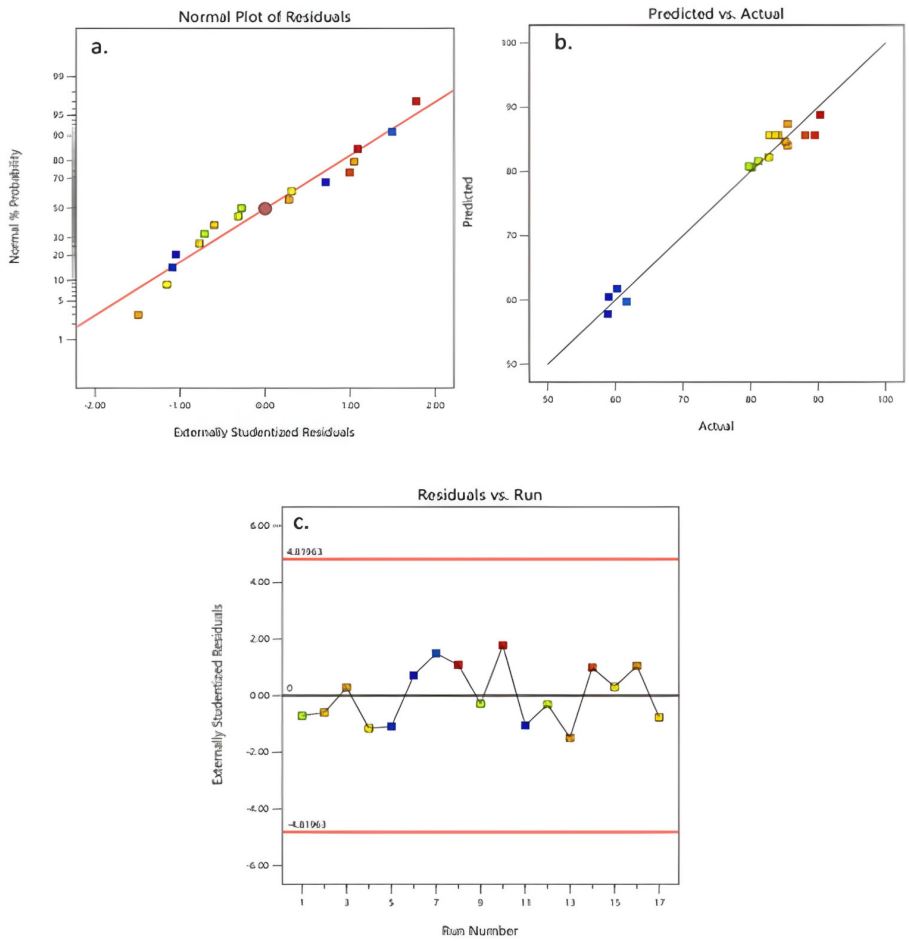

Figure 6. Diagnostic plots of the quadratic RSM model: (a) normal probability plot of residuals, (b) predicted versus experimental values, and (c) residuals versus run order

response (Equation 4). The indications of the regression coefficients provide information about the role of each variable and their interactions, with positive coefficients indicating factors that improve adsorption and negative values indicating factors that inhibit responsiveness (Salari, 2022). The addition of quadratic factors emphasizes the nonlinear nature of the adsorption process, enabling the employment of a quadratic response surface model for optimization (Kalebić et al., 2023).

$$\begin{aligned} \%\, Adsorption = {} & 85.65 - 0.8013A + \\ & + 12.80B - 1.17C - 1.81AB + 0.3483AC - \\ & - 2.13BC - 0.5888A^2 - 11.35B^2 - 2.85C^2 \end{aligned} \quad (4)$$

The ANOVA results in Table 6 show that the established quadratic model gives a statistically robust description of CIP adsorption on GO. The model has a high F-value of 27.56 and a matching p-value of 0.0001, indicating that the regression is highly significant and accounts for a substantial portion of the response variability. The relatively low residual contribution and non-significant lack-of-fit value ($p = 0.5932$) show that the model accurately represents the experimental behavior without systematic deviation, confirming its applicability for response surface analysis and prediction in the studied domain (Aman et al., 2023).

The adsorption process is dominated by GO mass (B) with an F-value of 164.94 and a p-value < 0.0001. This substantial statistical weight demonstrates that adsorbent availability is the key determining factor for CIP removal, as predicted by adsorption theory, which states that the number of available active sites directly influences absorption capacity. In contrast, the linear contributions of pH (A) and contact duration (C) are statistically negligible ($p = 0.4060$ and 0.2721, respectively), showing that within the studied ranges, these variables do not independently drive adsorption to the same extent as adsorbent mass. As a result, their influence is subtler, modulating rather than determining adsorption behavior (Wang et al., 2021).

The interaction terms (AB, AC, and BC) are not statistically significant ($p > 0.05$), indicating

Table 6. Analysis of variance (ANOVA) results for the quadratic RSM model of CIP adsorption

Source	Sum of squares	Df	Mean square	F-value	p-value
Model	1927.60	9	214.18	27.56	0.0001*
A – pH	6.07	1	6.07	0.78	0.4060
B – GO mass	1281.61	1	1281.61	164.94	< 0.0001*
C – Contact time	11.04	1	11.04	1.42	0.2721
AB	9.24	1	9.24	1.19	0.3117
AC	0.53	1	0.53	0.07	0.8016
BC	18.06	1	18.06	2.32	0.1712
A^2	1.13	1	1.13	0.15	0.7139
B^2	543.82	1	543.82	69.99	< 0.0001*
C^2	34.02	1	34.02	4.38	0.0747
Residual	54.39	3	18.13	—	—
Lack of fit	18.96	4	4.74	0.71	0.5932

Note: * significant.

that pairwise coupling between variables does not play a major role under the conditions investigated. The quadratic term for GO mass (B^2) is extremely significant ($F = 69.99$, $p < 0.0001$), indicating considerable curvature effects caused by non-linear adsorption behavior. This discovery demonstrates the saturation phenomenon, in which increasing adsorbent mass above a particular threshold results in declining advances in adsorption efficiency. The quadratic terms for pH (A^2) and contact time (C^2) have less influence, but C^2 makes a substantial contribution ($F = 4.38$, $p = 0.0747$), showing the onset of non-linearity at extended contact times (Gadre and Ritter, 2002). Overall, these findings demonstrate that CIP adsorption onto GO is primarily regulated by adsorbent mass, which has significant non-linear properties, with pH and contact time serving as secondary tuning parameters that refine performance rather than completely control it.

Table 7 summarizes statistical indications that support the quadratic model's robustness and reliability in describing CIP adsorption. The low standard deviation (2.79) relative to the mean answer (78.72) suggests that the experimental results are densely packed, whereas the coefficient of variation (3.54%) implies great precision and consistency across experimental runs. These metrics are consistent with the ANOVA results, which show a statistically significant model with a non-significant lack-of-fit, indicating that the observed variability is effectively described by the regression (Gadre and Ritter, 2002).

Table 7. Statistical performance indicators of the quadratic RSM model for CIP adsorption

Statistic	Value
Standard deviation	2.79
Mean response	78.72
Coefficient of variation (C.V., %)	3.54
R^2	0.9726
Adjusted R^2	0.9373
Predicted R^2	0.8190
Adequate precision	14.49

The model accurately explains and predicts CIP adsorption, with a high R^2 value of 0.9726. It accounts for nearly 97% of the change. Adjusted R^2 (0.9373) and projected R^2 (0.8190) are well aligned, indicating model stability and predictability without overfitting. Furthermore, the precision value of 14.49, significantly higher than the suggested threshold of 4, indicates a high signal-to-noise ratio and verifies that the model provides adequate resolution for successful design space navigation and CIP adsorption performance optimization (Ahmed et al., 2024).

Interaction effects in process variables and their influence on CIP % adsorption

Figures 7 (a,b) show the interaction between pH and GO mass at a given contact duration of 35 minutes, demonstrating a strong nonlinear response surface. The center point at pH 5 and 30 mg GO has an adsorption efficiency of about 88%, indicating near-optimal circumstances. Adsorption declines dramatically to 58% under very acidic circumstances (pH 2) with a low GO

mass of 10 mg, demonstrating that CIP uptake is limited by insufficient adsorbent availability. At the same pH, adding 50 mg of GO increases adsorption to around 90%, indicating that adsorbent dose has a bigger influence than pH. This trend demonstrates the dominant importance of GO mass in supplying accessible active sites, even under less favorable pH circumstances, and it is consistent with the ANOVA analysis's finding of a large quadratic effect.

Figures 7 (c,d) show the pH-contact time interaction, which has a rather uniform response surface when compared to other interactions. The center point at pH 5 and 35 min corresponds to an adsorption efficiency of about 88%, although the strong yellow-orange regions in the contour plot indicate a very homogenous adsorption response across a wide range of circumstances. Adsorption is reduced to around 59% under extreme conditions (pH 2 and 10 min contact duration), demonstrating that very acidic surroundings combined with short contact times are detrimental for CIP adsorption. The comparatively moderate surface curvature implies that pH and contact duration are secondary characteristics that affect adsorption rather than directly controlling it.

The interaction between GO mass and contact time (Figure 7 (e,f)) shows a more significant curved response surface, indicating saturation effects at larger adsorbent dosages. Adsorption reaches roughly 88% at the central point (30 mg GO, 35 min). Increasing the GO mass to 30-50 mg yields consistently high adsorption efficiencies, but smaller masses (10-20 mg) result in significantly lower adsorption rates. For 10 mg GO, extending the contact time from 10 to 60 minutes

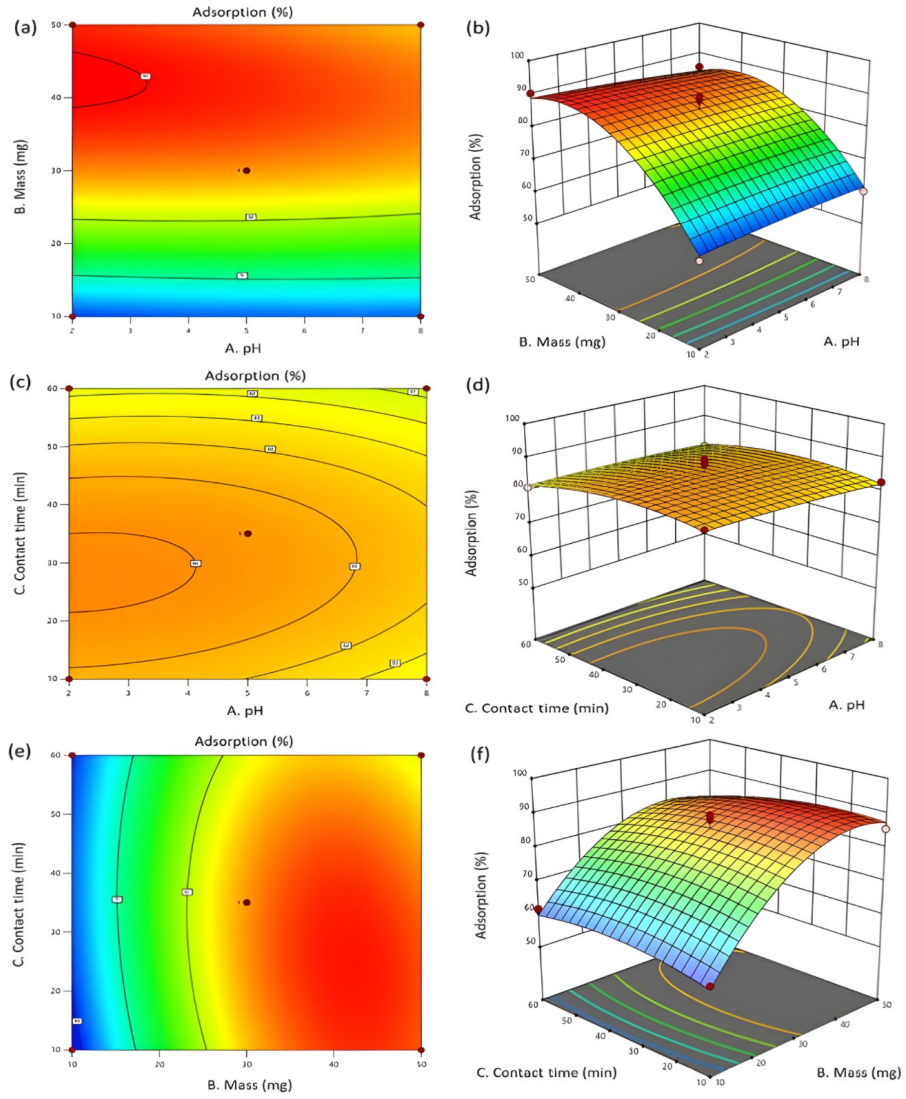

Figure 7. Contour (2D) and response surface (3D) plots illustrating the interactive effects of GO mass–pH (a, b), pH–contact time (c, d), and contact time–GO mass (e, f) on CIP adsorption performance

only marginally increases adsorption from 58% to 61%, indicating that longer contact times cannot make up for a low adsorbent mass. At 50 mg GO, adsorption reduces from ≈85% at 10 min to ≈79% at 60 min, indicating saturation and potential aggregation effects that limit surface usage. This tendency is consistent with previous findings published by Sikri et al. (Sikri et al., 2025), who found decreasing efficiency beyond the optimal GO dosage due to active site obstruction.

Validation of experiment using RSM confirmation test on % CIP adsorption

A confirmation test was conducted to validate the reliability of achieving the optimal conditions forecasted by the RSM model in practice. This step is very important to confirm that the statistically optimized parameters lead to consistent experimental results and that the model's predictions are within an acceptable range of error (Zewide et al., 2025). This atudy utilized the desirability function methodology for optimization, wherein the desirability value (D) signifies the model's comprehensive capacity to concurrently fulfill all specified optimization criteria. A desirability value near one indicates the attainment of the optimization objective (Fernandi et al., 2015).

The ramp desirability plot in Figure 8 shows that a desirability value of 1.000 was reached. This means that the answer was the best and most fair. Design Expert 13.0 came up with 100 possible answers, and number 3 was chosen as the best one. The ideal situation has a pH of 3.16, a GO mass of 43.00 mg, and a contact time of 29.94 minutes. Around 90.46% of the time, CIP adsorption is expected to work. This ideal point is vital because it is in the center of the experimental area. The result means that the answer is strong and stable enough to use in real life (Cho, et al., 2006).

The improved conditions are consistent with the previously stated adsorption mechanisms. A slightly acidic pH promotes the adhesion of CIP molecules to the oxygen-containing functional groups on the GO surface. The GO mass is also high enough to ensure that molecules have adequate locations to stick. The moderate contact time also demonstrates that adsorption equilibrium can be achieved rapidly, implying that the extraction procedure does not have to take longer than necessary. The confirmation test and desirability analysis demonstrate that the RSM model is statistically valid and useful in the real world. This implies that employing GO in DSPE applications to improve CIP adsorption is a beneficial idea (Thorisingam and Mustafa, 2022).

Table 8 shows the results of the confirmation test that was done to check how accurate and reliable the RSM model's anticipated conditions for CIP adsorption were. The model projected an adsorption effectiveness of 90.46% under the best operating conditions; however, the actual average adsorption was only 88.39%. The experimental value is very close to the 95% prediction interval (85.77–95.15%). This shows that the model prediction is statistically compatible with the actual experimental response (Hashemi et al., 2025).

The relatively small percentage error of 2.34%, which is far lower than the usual 5% criterion, shows that the anticipated and experimental

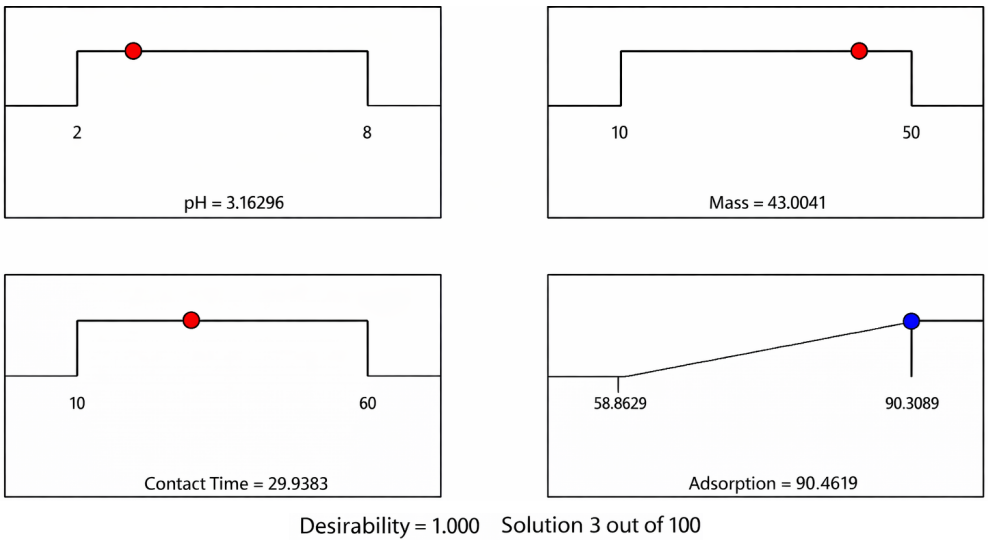

Figure 8. Ramp desirability plot for CIP adsorption optimization using GO

Table 8. Results of the confirmation test for CIP adsorption optimization using GO

Response	Predicted value (%)	95% PI (lower) (%)	Experimental mean (%)	95% PI (upper) (%)	Error (%)
CIP adsorption	90.46	85.77	88.39	95.15	2.34

findings are quite close to each other. This small difference shows that the quadratic model not only shows the general trend of adsorption, but it also makes accurate point predictions when conditions are right (Roy, 2022). The RSM model is strong, and the small error margin shows that the assumptions made during its construction were correct, such as the factors chosen and how they relate to each other.

Slight variation exists between anticipated and observed adsorption values because experiments are imperfect. For example, small changes in the parameters of the solution or the dispersion of the adsorbent are unavoidable in adsorption studies. The prediction and confirmation are so close that the optimized conditions are statistically accurate and can be repeated in the lab (Bbumba et al., 2024). The confirmation test shows that the RSM model that was made is good for guiding optimization and scale-up decisions on CIP adsorption utilizing GO in DSPE applications.

CONCLUSIONS

Graphene oxide derived from sugarcane bagasse was successfully synthesized using a simple and ecologically friendly method, indicating that agricultural waste may be converted into a valuable functional material for analytical applications. Structural and surface investigations showed the existence of numerous oxygen-containing functional groups, increased interlayer spacing, and a defect-rich morphology, all of which contribute to the high adsorption affinity for CIP molecules.

The DSPE process was optimized using RSM, which demonstrated that adsorbent mass is the most important element in determining CIP adsorption, while solution pH and contact duration act as complementary factors in modulating adsorption efficiency. The quadratic model demonstrated great statistical validity, as evidenced by high explanatory power, consistent predictive performance, and well-behaved residual diagnostics. Response surface analysis revealed nonlinear behavior and adsorption saturation effects at greater GO loadings, underlining the need for balanced operating conditions.

The adjusted DSPE conditions resulted in high adsorption efficiency with great agreement between predicted and experimental findings, with a low prediction error of 2.34%, demonstrating the model's robustness and practical reliability. This study shows that biomass-derived GO can be used as an efficient, low-cost, and long-lasting adsorbent for DSPE-based antibiotic analysis. The proposed approach offers a viable foundation for ecologically responsible analytical extraction and can be applied to the detection of additional developing pollutants in aquatic settings.

Acknowledgements

The authors express their gratitude to the University of Lampung for the financial assistance provided through the Professorship Program (Contract Nos. 2077/UN26.21/PN/2025) under the DIPA funding scheme. The authors also thank all individuals and institutions for their significant contributions to this study.

REFERENCES

1. Ahmed, Y., Maya, A. A. S., Akhtar, P., Alam, M. S., others. (2024). A novel interpretable machine learning and metaheuristic-based protocol to predict and optimize ciprofloxacin antibiotic adsorption with nano-adsorbent. *Journal of Environmental Management, 370*, 122614. https://doi.org/10.1016/j.jenvman.2024.122614
2. Ahmmed, M. S., Mohiuddin, A. K. (2024). Highly effective removal of ciprofloxacin from aqueous solution using graphene oxide functionalized zeolite. *Journal of Engineering Science, 15*(2), 29–39. https://doi.org/10.3329/jes.v15i2.82160
3. Aman, A. M. N., Selvarajoo, A., Lau, T. L., Chen, W. H. (2023). Optimization via response surface methodology of palm kernel shell biochar for supplementary cementitious replacement. *Chemosphere, 313*, 137477. https://doi.org/10.1016/j.chemosphere.2022.137477
4. Anggraini, V., Dassanayake, S., Emmanuel, E., Yong, L. L., Kamaruddin, F. A., Syamsir, A. (2023).

Response surface methodology: The improvement of tropical residual soil mechanical properties utilizing calcined seashell powder and treated coir fibre. *Sustainability, 15*(4), 3588. https://doi.org/10.3390/su15043588

5. Ariyanti, D., Lesdantina, D., Satriadi, H. (2021). Synthesis and characterization of graphene-like material derived from sugarcane bagasse. *IOP Conference Series: Materials Science and Engineering, 1053*(1), 012013. https://doi.org/10.1088/1757-899X/1053/1/012013
6. Bansal, O. P. (2022). Antibiotics in the environment: A review. *International Journal of Frontiers in Biology and Pharmacy, 2*, 57–83. https://doi.org/10.53294/ijfbpr.2022.2.1.0030
7. Barathe, P., Kaur, K., Reddy, S., Shriram, V., Kumar, V. (2024). Antibiotic pollution and associated antimicrobial resistance in the environment. *Journal of Hazardous Materials Letters, 5*, 100105. https://doi.org/10.1016/j.hazl.2024.100105
8. Bbumba, S., Kigozi, M., Nabatanzi, J., Karume, I., others. (2024). Response surface methodology: A review on optimization of adsorption studies. *Asian Journal of Chemical Sciences, 14*(6), 106–113. https://doi.org/10.9734/ajocs/2024/v14i6338
9. Buhani, M., Pratama, D. S., Suharso, Rinawati. (2017). Modification of Chaetoceros sp. biomass with silica–magnetite coating and adsorption studies towards Cu(II) ions in single and binary system. *Asian Journal of Chemistry, 29*, 2734–2738. https://doi.org/10.14233/ajchem.2017.20859
10. Cardoso, A. T., Martins, R. O., Lanças, F. M. (2024). Advances and applications of hybrid graphene-based materials as sorbents for solid phase microextraction techniques. *Molecules, 29*(15), 3661. https://doi.org/10.3390/molecules29153661
11. Çalışkan Salihi, E., Wang, J., Kabacaoğlu, G., Kırkulak, S., Šiller, L. (2021). Graphene oxide as a new generation adsorbent for the removal of antibiotics from waters. *Separation Science and Technology, 56*(3), 453–461. https://doi.org/10.1080/01496395.2020.1717533
12. Challa, A. A., Saha, N., Ngwabebhoh, F. A., Nguyen, H. T., Urbánek, P., Fei, H., Saha, P. (2022). Synthesis and characterization of graphene oxide from residual biomass. In *2022 IEEE 12th International Conference Nanomaterials: Applications & Properties (NAP)* (pp. 1–4). https://doi.org/10.1109/NAP55339.2022.9934117
13. Darmawan, I., Wannasen, L., Pinitsoontorn, S. (2024). Synthesis, characterization, and electrochemical properties of reduced graphene oxide produced from sugarcane bagasse for supercapacitor applications. *Biointerface Research in Applied Chemistry, 14*, 109. https://doi.org/10.33263/BRIAC145.109
14. David, V., Galaon, T., Bacalum, E. (2019). Sample enrichment by solid-phase extraction for reaching parts per quadrillion levels in environmental analysis. *Chromatographia, 82*(8), 1139–1150. https://doi.org/10.1007/s10337-019-03696-y
15. Edward, K., Mamun, K., Narayan, S., Assaf, M., Rohindra, D., Rathnayake, U. (2023). State-of-the-art graphene synthesis methods and environmental concerns. *Applied and Environmental Soil Science, 2023*, 8475504. https://doi.org/10.1155/2023/8475504
16. Fernandi, M., Baroni, M., Bazzurri, M., Benedetti, P., others. (2015). The CARSO (Computer Aided Response Surface Optimization) procedure in optimization studies. *Applied Mathematics, 6*(11), 1947–1956. https://doi.org/10.4236/am.2015.611172
17. Gadre, S. A., Ritter, J. A. (2002). New model for nonlinear adsorption and diffusion based on a quartic concentration profile approximation. *Industrial & Engineering Chemistry Research, 41*(17), 4353–4361. https://doi.org/10.1021/ie020197z
18. Gupta, V. K., Agarwal, S., Asif, M., Fakhri, A., Sadeghi, N. (2017). Application of response surface methodology to optimize the adsorption performance of a magnetic graphene oxide nanocomposite adsorbent for removal of methadone from the environment. *Journal of Colloid and Interface Science, 497*, 193–200. https://doi.org/10.1016/j.jcis.2017.03.006
19. Hagarová, I., Nemček, L. (2024). Analytical application of layered double hydroxides as high-capacity sorbents in dispersive solid phase extraction for the separation and preconcentration of (ultra) trace heavy metals. *Critical Reviews in Analytical Chemistry, 54*(8), 3114–3127. https://doi.org/10.1080/10408347.2023.2227906
20. Hashemi, S. Y., Akbari, H., Raei, M., Adibzadeh, A. (2025). Application of response surface methodology (RSM) in optimisation of levofloxacin and ciprofloxacin removal by NH_2/MOF: Kinetics and isotherm study. *International Journal of Environmental Analytical Chemistry, 105*(4), 856–879. https://doi.org/10.1080/03067319.2023.2275608
21. Imam, S. S., Adnan, R., Mohd Kaus, N. H., Us Saqib, N. (2023). Influence of various operational parameters on the photocatalytic degradation of ciprofloxacin in aqueous media: A short review. *Toxin Reviews, 42*(3), 655–670. https://doi.org/10.1080/15569543.2023.2213319
22. Kalebić, B., Bafti, A., Cajner, H., Marciuš, M., Matijašić, G., Ćurković, L. (2023). Optimization of ciprofloxacin adsorption on clinoptilolite-based adsorbents using response surface methodology. *Nanomaterials, 13*(4), 740. https://doi.org/10.3390/nano13040740
23. Laçin, Ö. (2022). Yeni bir yaklaşımla elde edilen grafen oksit sentezlerinde SEM ve TEM analizleri (in Turkish). *Avrupa Bilim ve Teknoloji Dergisi, 39*,

76–79. https://doi.org/10.31590/ejosat.1137870

24. Lajqi Berisha, N., Poceva Panovska, A., Hajrulai-Musliu, Z. (2024). Antibiotic resistance and aquatic systems: Importance in public health. *Water, 16*(17), 2362. https://doi.org/10.3390/w16172362
25. Li, L., Tang, Y., Bao, Z., Tu, W., Peng, L., others. (2024). When graphene meets circular agriculture: Insights into agricultural sustainable development. *Biosystems Engineering, 237*, 92–117. https://doi.org/10.1016/j.biosystemseng.2023.12.002
26. Li, Z., Xu, F., Liu, Z., Qin, C., Ren, H., Li, Y. (2018). Facile synthesis of novel porous self-assembling hydrogen-bonding covalent organic polymers and their applications towards fluoroquinolone antibiotics adsorption. *RSC Advances, 8*(58), 33516–33522. https://doi.org/10.1039/C8RA06806B
27. Mohamed, K. M., Vijaya, J. J., Winston, A. J. P. P., Akash, K., Sagayaraj, P., Rajeshkumar, S., Al-Sadoon, M. K. (2024). Untapped potential: Sugarcane bagasse to biocompatible graphene oxide as biomedicine. *Diamond and Related Materials, 148*, 111479. https://doi.org/10.1016/j.diamond.2024.111479
28. Mubarak, A. A., Ilyas, R. A., Nordin, A. H., Ngadi, N., Alkbir, M. F. M. (2024). Recent developments in sugarcane bagasse fibre-based adsorbent and their potential industrial applications: A review. *International Journal of Biological Macromolecules, 277*, 134165. https://doi.org/10.1016/j.ijbiomac.2024.134165
29. Nishina, Y. (2024). Mass production of graphene oxide beyond the laboratory: Bridging the gap between academic research and industry. *ACS Nano, 18*(49), 33264–33275. https://doi.org/10.1021/acsnano.4c13297
30. Öner, M., Demir, C., Çetin, G., Bakırdere, S. (2023). Development of a rapid and efficient analytical method for trace lead determination: Manganese dioxide nanoflower-based dispersive solid-phase extraction. *Measurement, 211*, 112606. https://doi.org/10.1016/j.measurement.2023.112606
31. Podder, S., Mukherjee, S. (2024). Response surface methodology (RSM) as a tool in pharmaceutical formulation development. *Asian Journal of Pharmaceutical and Clinical Research, 17*(11), 18–25. https://doi.org/10.22159/ajpcr.2024v17i11.52149
32. Poonpat, P., Uwanno, T., Tajorn, V., Bodsayawit, S., Reilly, M. P., Wongwiriyapan, W. (2025). Eco-friendly synthesis of reduced graphene oxide from agricultural waste for electrodes in capacitive deionization applications. *Journal of Physics: Conference Series, 2934*(1), 012003. https://doi.org/10.1088/1742-6596/2934/1/012003
33. Rinawati, R., Buhani, B., Widiarti, W., Isro, A., Fitrianingsih, E., others. (2024). Enhancing ciprofloxacin removal: Unveiling the potential of graphene oxide synthesized from cassava peels through Box–Behnken design optimization. *Journal of Sustainable Development of Energy, Water and Environment Systems, 12*(4), 1–20. https://doi.org/10.13044/j.sdewes.d12.0516 (a)
34. Rinawati, R., Kiswandono, A. K., Widiarto, S., Kasih, Y. O., Hadi, S. (2023). Study on activated carbon derived from cassava peels as magnetic solid of dispersive solid phase extraction technique for determination of tetracycline. *Research Journal of Chemistry and Environment, 27*(3), 1–8. https://doi.org/10.25303/2703rjce01008 (b)
35. Roy, P. (2022). Adsorptive removal of hexavalent chromium using response surface methodology and artificial neural network. *Rasayan Journal of Chemistry, 15*(2), 1145–1153. https://doi.org/10.31788/RJC.2022.1526930
36. Salari, M. (2022). Optimization by Box–Behnken design and synthesis of magnetite nanoparticles for removal of the antibiotic from an aqueous phase. *Adsorption Science & Technology, 2022*, 1267460. https://doi.org/10.1155/2022/1267460
37. Sayfo, S., Alshameri, A., Ibrahim, A. (2023). Physicochemical properties of biochar and activated carbon derived from biomass residues. *ACS Omega, 8*(15), 13874–13888. https://doi.org/10.1021/acsomega.3c01234
38. Sharma, A. (2025). Pharmaceutical pollution in aquatic ecosystems: Impacts and bioremediation strategies. *Geography, Earth Science and Environment: Research Highlights, 4*, 140–148. https://doi.org/10.9734/bpi/geserh/v4/4035
39. Shukri, D. S. M., Yahaya, N., Miskam, M., Yusof, R., others. (2023). Advances in dispersive solid-phase extraction techniques for analytical quantification of fluoroquinolone antibiotics. *Microchemical Journal, 193*, 109154. https://doi.org/10.1016/j.microc.2023.109154
40. Sikri, N., Kumar, S., Behera, B., Mehta, J. (2025). Graphene oxide/layered double hydroxide composite as highly efficient and recyclable adsorbent for removal of ciprofloxacin from aqueous phase. *Frontiers in Nanotechnology, 7*, 1578620. https://doi.org/10.3389/fnano.2025.1578620
41. Silva, W. C. H., Zafar, M. A., Allende, S., Jacob, M. V., Tuladhar, R. (2024). Sustainable synthesis of graphene oxide from waste sources: A comprehensive review of methods and applications. *Materials Circular Economy, 6*(1), 23. https://doi.org/10.1007/s42824-024-00117-w
42. Silveira, G. D. O., Pego, A. M. F., Pereira e Silva, J., Yonamine, M. (2019). Green sample preparations for the bioanalysis of drugs of abuse in complex matrices. *Bioanalysis, 11*(4), 295–312. https://doi.org/10.4155/bio-2018-0208
43. Socas-Rodríguez, B., Herrera-Herrera, A. V., Asensio-Ramos, M., Hernández-Borges, J.

(2015). Dispersive solid-phase extraction. *Analytical Separation Science*, 1525–1570. https://doi.org/10.1002/9783527678129.assep056

44. Taghvimi, A., Dastmalchi, S., Javadzadeh, Y. (2020). Application of carbonic nanosheets based on urea precursors as dispersive solid phase extraction adsorbent for extraction of methamphetamine from urine samples. *Advanced Pharmaceutical Bulletin, 11*(4), 624–631. https://doi.org/10.34172/apb.2021.071
45. Tamilselvi, R., Ramesh, M., Lekshmi, G. S., Bazaka, O., Levchenko, I., Bazaka, K., Mandhakini, M. (2020). Graphene oxide–based supercapacitors from agricultural wastes: A step to mass production of highly efficient electrodes for electrical transportation systems. *Renewable Energy, 151*, 731–739. https://doi.org/10.1016/j.renene.2019.11.072
46. Thangaraj, B., Mumtaz, F., Abbas, Y., Anjum, D. H., Solomon, P. R., Hassan, J. (2023). Synthesis of graphene oxide from sugarcane dry leaves by two-stage pyrolysis. *Molecules, 28*(8), 3329. https://doi.org/10.3390/molecules28083329
47. Thorisingam, Y., Mustafa, M. S. (2022). Augmented approach to desirability function based on principal component analysis. *International Journal of Academic Research in Progressive Education and Development, 11*(2), 526–533.
48. Torgbo, S., Quan, V. M., Sukyai, P. (2021). Cellulosic value-added products from sugarcane bagasse. *Cellulose, 28*(9), 5219–5240. https://doi.org/10.1007/s10570-021-03918-3
49. Umeh, C. T., Nduka, J. K., Akpomie, K. G., Ighalo, J. O., Mogale, R. (2025). Adsorptive effect of corn silk-loaded nickel oxide and copper oxide nanoparticles for elimination of ciprofloxacin from wastewater. *ACS Omega, 10*(4), 3784–3800. https://doi.org/10.1021/acsomega.4c09192
50. Wang, Q., Yang, M., Qi, X., Wang, J., Sun, K., Li, Z., Deng, G. (2021). A novel graphene oxide decorated with halloysite nanotubes (HNTs/GO) composite used for the removal of levofloxacin and ciprofloxacin in a wide pH range. *New Journal of Chemistry, 45*(39), 18315–18326. https://doi.org/10.1039/D1NJ03807A
51. Wang, W., Weng, Y., Luo, T., Wang, Q., Yang, G., Jin, Y. (2023). Antimicrobial and the resistances in the environment: Ecological and health risks, influencing factors, and mitigation strategies. *Toxics, 11*(2), 185. https://doi.org/10.3390/toxics11020185
52. Yadav, S., Goel, N., Kumar, V., Tikoo, K., Singhal, S. (2018). Removal of fluoroquinolone from aqueous solution using graphene oxide: Experimental and computational elucidation. *Environmental Science and Pollution Research, 25*(3), 2942–2957. https://doi.org/10.1007/s11356-017-0596-8
53. Yakamercan, E., Aygün, A., Simsek, H. (2024). Antibiotic ciprofloxacin removal from aqueous solutions by electrochemically activated persulfate process: Optimization, degradation pathways, and toxicology assessment. *Journal of Environmental Sciences, 143*, 85–98. https://doi.org/10.1016/j.jes.2023.08.013
54. Yang, X., Liu, J., Wang, Y., Zhang, L., Chen, H. (2022). Nonmetal functional groups of biochar for pollutants removal: A review. *Environmental Functional Materials, 2*(3), 118–138. https://doi.org/10.1016/j.hazadv.2022.100171
55. Zewide, Y. T., Yemata, T. A., Ayalew, A. A., Kedir, H. J., others. (2025). Application of response surface methodology (RSM) for experimental optimization in biogenic silica extraction from rice husk and straw ash. *Scientific Reports, 15*(1), 132. https://doi.org/10.1038/s41598-024-83724-6
56. Zhao, W., Hao, C., Guo, Y., Shao, W., Yimwi, T., Zhao, P. (2023). Optimization of adsorption conditions using response surface methodology for tetracycline removal by $MnFe_2O_4$/multi-wall carbon nanotubes. *Water, 15*(13), 2392. https://doi.org/10.3390/w15132392